International Journal of Mass Spectrometry 282 (2009) 133–140

Contents lists available at ScienceDirect

International Journal of Mass Spectrometry

journal homepage: www.elsevier.com/locate/ijms

Low-energy electron-induced chemistry of condensed-phase hexamethyldisiloxane: Initiating dissociative process and subsequent reactions

I. Ipolyi [a], E. Burean [a], T. Hamann [a], M. Cingel [b], S. Matejcik [b], P. Swiderek [a,*]

[a] Universität Bremen, Fachbereich 2 (Chemie/Biologie), Leobener Straße/NW 2, Postfach 330440, 28334 Bremen, Germany
[b] Department of Experimental Physics, Comenius University, Mlynska dolina F2, 84248 Bratislava, Slovakia

ARTICLE INFO

Article history:
Received 23 January 2009
Received in revised form 20 February 2009
Accepted 23 February 2009
Available online 6 March 2009

Keywords:
Electron-induced reactions siloxanes
Thermal desorption spectrometry
Dissociative electron attachment

ABSTRACT

Thin films of condensed hexamethyldisiloxane (HMDSO) have been exposed to electron irradiation at incident energies between 5 and 15 eV and analysed afterwards by thermal desorption spectrometry (TDS). Formation of products is observed at energies at and above 11 eV and quantified at 15 eV by comparison with reference samples of known composition. Gas-phase measurements aiming at detection of dissociative electron attachment (DEA) were, in addition, performed to obtain more insight into the dominant electron-induced dissociation channel expected to initiate further reactions in the condensed phase.

Apart from CH_4 which is the most obvious product present in exposed films of HMDSO, tetramethylsilane (TMS) and smaller amounts of C_2H_6 have been detected. The quantity of the products is by one to two orders of magnitude smaller than the amount of decomposed HMDSO. In addition, signals ascribed to unquantified amounts of larger siloxanes have been observed. The present results together with previous gas-phase results from literature suggest that dissociative ionisation leading to Si–C bond rupture and release of a methyl radical is the most important electron-driven initial reaction step. Possible mechanisms of the subsequent reactions induced by the fragments of the initial dissociation reaction are reviewed and discussed in relation to the observed product quantities.

1. Introduction

Low-energy electrons offer the prospect of modifying surfaces or thin films by inducing chemical reactions [1–4]. The outcome of such reactions can, in principle, be controlled by proper tuning of the energy of electrons incident onto a molecule or a surface. A fine example demonstrating this selectivity has been provided by recent in-depth investigations of electron-induced reactions in gaseous thymine [5]. However, to use this selectivity for the controlled modification of materials, one must consider and identify any changes in the reaction pathways or reaction rates including new reaction channels, which may occur upon transition to the condensed phase.

Hexamethyldisiloxane (HMDSO $(CH_3)_3SiOSi(CH_3)_3$) is commonly used in plasma processes for the deposition of silicon oxide films. Diluted with oxygen and a noble gas, it is used as replacement for the explosive monomer silane (SiH_4) [6]. In such plasma processes, low-energy electrons contribute to the formation of reactive species which then lead to SiO_2 film growth at a surface. Therefore, the reactions of HMDSO in plasmas [6–11] and also under exposure of the vapour to low-energy electrons [12] have been studied previously. Also, the dissociative excitation and the optical emissions of HMDSO under electron impact were investigated [13,14]. However, as reported for tetraethylorthosilicate (TEOS, $Si(OC_2H_5)_4$) [15] using electron beam techniques, similar reactions may also be initiated directly at a surface to grow solid films. Similarly, a thin condensed film of HMDSO or, alternatively, oligo- or polysiloxanes, may be processed using electron irradiation [16]. Electron-induced reactions could thus be an interesting new approach for the fabrication of cross-linked or even patterned surfaces based on siloxane materials.

To understand electron-induced chemical processes in siloxanes and thus learn to control the chemical modification and properties of these materials, we have chosen as a model system, to investigate HMDSO condensed onto a surface at low temperature. Using thermal desorption spectrometry (TDS), it was previously observed that thin multilayer films of HMDSO show two desorption maxima of which the higher temperature one decays more rapidly under electron exposure [16]. On the other hand, the cross-section for depletion of HMDSO deduced from these data was surprisingly similar to values obtained in the gas-phase [12]. In order to analyse the relation between the known gas-phase processes occurring under single electron collision conditions including subsequent ion-molecule reactions and the reactions observed in the

* Corresponding author.
E-mail address: swiderek@uni-bremen.de (P. Swiderek).

1387-3806/$ – see front matter © 2009 Elsevier B.V. All rights reserved.
doi:10.1016/j.ijms.2009.02.020

condensed phase under continued exposure to electrons, a more comprehensive search for reaction products and estimate of their amount is presented here. This includes a search for dissociative electron attachment (DEA) channels in gaseous HMDSO. Besides dissociative ionisation that has been reported in detail [12] DEA is a potential initiating process that may lead to further reactions in the condensed phase. Such processes are often effective at energies considerably below the ionisation threshold and thus are promising with respect to controlling the chemical changes.

The previous results on dissociative ionisation of gaseous HMDSO under electron impact report a threshold of 10 eV and a steadily increasing cross-section up to 70 eV [12]. The present condensed phase experiments use incident electron energies (E_0) ranging from 5 to 15 eV to examine if the ionisation threshold affects the reactions in condensed HMDSO in a similar way. In addition, gas-phase experiments aiming at DEA were performed at incident electron energies between 0 and 15 eV. This allows us to evaluate the significance of ionisation processes as initiating reaction as compared to other reactive pathways and, more specifically, DEA as well as dipolar dissociation (DD). By comparison with the desorption temperatures of films of known composition, the products formed in the condensed phase are identified and quantified at E_0 = 15 eV where the reaction rate is highest. The low temperature at which electron exposure takes place allows us to trap volatile species such as CH_4, C_2H_6, and tetramethylsilane (TMS). Furthermore, formation of larger siloxanes is observed and indicates that oligomerisation reactions take place. Possible mechanisms are discussed in relation with previously described ion-molecule reactions in the gas-phase [8,12] and electron-induced reactions in condensed molecular films [17].

2. Experimental

Experiments aiming at the detection of negative ions formed by electron attachment to HMDSO in the gas phase have been performed using the crossed electron/molecule beams technique at Comenius University described in detail previously [18]. The apparatus is able to detect all negative ions in the mass range from 2 to 2000 amu with high sensitivity due to the use of the pulse counting technique. The H^- ion was thus out of range of the experiment due to mass range limitation of the mass spectrometer. The experiments were performed in the electron energy range from about 0 up to 15 eV. HMDSO used for the gas-phase experiments was purchased from Merck with stated purity >99%.

The condensed phase experiments were performed in Bremen using an ultrahigh vacuum (UHV) setup described in detail previously [17]. It is pumped to a pressure of 10^{-10} Torr by a turbomolecular pump and occasional use of a titanium sublimator. Molecular films were grown on a polycrystalline Au substrate held at 35 K by means of a closed-cycle He cryostat. The growth as well as low-energy electron-induced reactions in these samples at the same temperature were then monitored by thermal desorption spectrometry at a heating rate of 1 K/s. For this a Quadrupole Mass Spectrometer (QMS) residual gas analyser (Stanford, 200 amu) with electron impact ionisation at 70 eV was used.

A commercial flood gun delivering currents of the order of a few $\mu A/cm^2$ as measured at the sample was used for electron exposure. The non-monochromatized electron beam has an estimated resolution of the order of 0.5–1 eV. The energies stated here (E_0) are the nominal values as set by the power supply. At E_0 = 15 eV an exposure of 2000 μC was obtained within 2 min. Charging effects that may somewhat change the incident energy at the sample are not taken into account here for reasons explained previously [17].

Hexamethyldisiloxane (HMDSO) and tetramethylsilane (TMS, $Si(CH_3)_4$) were purchased from ABCR at stated purities of 99.9% and 99.9% (NMR grade). Octamethyltrisiloxane (OMTSO $(CH_3)_3SiOSi(CH_3)_2OSi(CH_3)_3$) was obtained from Aldrich (98%) and methane (CH_4, 99.995%) from Messer Griesheim. Liquids used for TDS measurements were degassed prior to use by repeated freeze–pump–thaw cycles in vacuum; the gas was used as received. For film deposition, vapours of pure HMDSO or mixtures of vapours were leaked onto the Au substrate via a gas-handling manifold consisting of precision leak valves and a small calibrated volume where the absolute pressure is measured with a capacitance manometer. The pressure drop in the manifold is used to measure the vapour quantity. The amount of vapour required for monolayer formation and thus also the average film thickness at higher deposited amounts of vapour could be estimated roughly from the thickness dependence of the TDS curves [16]. We conclude that an amount of vapour of 0.12 mTorr (±50%) produces a monolayer. All measurements presented here concern films with thickness well in the multilayer regime. Due to the large uncertainty we state in the figures only the vapour doses. Prior to each deposition, the substrate was cleaned by heating of two thin Ta ribbons spot-welded to the thicker Au substrate whereby the substrate reached 273 K to evaporate any material that would contribute to the next TDS scan.

In an exposure experiment, thermal desorption was induced after an irradiation time corresponding to a specific accumulated charge by increasing the substrate temperature from 35 up to 270 K at a typical rate of 1 K/s. TDS curves were recorded for up to four different masses, each being characteristic of a specific molecule. A few additional reflection-absorption infrared spectra (RAIRS) were obtained in situ using a Bruker 66 v/s spectrometer with MCT detector coupled directly to the UHV system.

3. Results and discussion

3.1. Search for dissociative electron attachment processes in gaseous HMDSO

The crossed electron/molecule beams experiments aiming at identifying DEA processes did not reveal any negative ions at incident electron energies between about 0 and 15 eV. Even measurements of the total ion current did not yield any measurable signal within the sensitivity of the experiment. This is in accord with previous results that also pointed towards a lack of negative ions in discharge and plasma experiments [11,19]. However due to the mass range limitation of the mass spectrometer, we are not able to exclude completely the formation of the H^- ions, as this ion is undetectable by the mass spectrometer.

While formation of H^- cannot be excluded with certainty from the present experiments, the results show that DEA leading to any other negative ion does not play an important role in the electron-induced reactions of HMDSO in the gas phase. Taking into account that the cross-section for formation of cationic fragments already reaches a value of 4.0×10^{-16} cm^2 at E_0 = 15 eV and the only important product at this E_0 is $[HMDSO–CH_3]^+$ [12], the lack of CH_3^- leads to the conclusion that also dipolar dissociation at the E_0 investigated here cannot be significant in gaseous HMDSO.

3.2. Energy dependence of low-energy electron-induced reactions in HMDSO films

Fig. 1 shows, for a HMDSO film produced from a vapour dose of 2 mTorr, TDS curves recorded at 147 amu, i.e., the most abundant fragment of HMDSO, prior to and after electron exposure of 500 μC at various E_0. The TDS curves show a characteristic signal with two maxima, assigned previously to two different solid phases of HMDSO, with the 149 and 158 K desorption signals corresponding to a disordered and a more ordered phase [16]. While

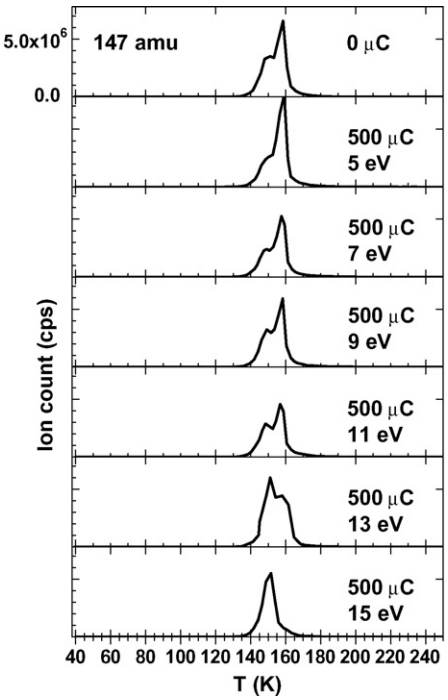

Fig. 1. Thermal desorption spectra of HMDSO multilayer films recorded at 147 amu ($[HMDSO–CH_3]^+$, the dominant fragment mass of HMDSO) prior to and after electron exposure of 500 μC at various incident energies. The HMDSO films were deposited at 35 K from amounts of vapour corresponding to a pressure drop in the inlet system of 2.0 mTorr.

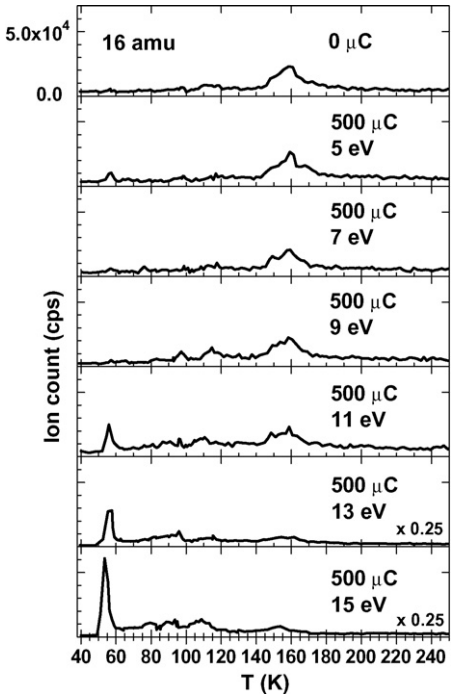

Fig. 2. Thermal desorption spectra of HMDSO multilayer films recorded at 16 amu (CH_4^+) prior to and after electron exposure of 500 μC at various incident energies during the same experiment as the data shown in Fig. 1.

the HMDSO signal is somewhat higher at E_0 = 5 eV, most likely due to a variation in film thickness and indicative of the margin of error inherent in the vapour dosing procedure, the HMDSO signal clearly starts to change at E_0 = 11 eV. Here, the 158 K maximum is somewhat reduced after electron exposure of 500 μC. The effect is more obvious at E_0 = 13 eV and becomes so strong at 15 eV that the high-temperature signal has already disappeared after an exposure of 500 μC as reported in the previous work [16].

The production of CH_4 at E_0 = 15 eV was demonstrated earlier [16,20]. CH_4 desorption is obvious from a sharp peak near 55 K and an additional sequence of signals extending to a temperature of about 160 K in the 16 amu curves (Fig. 2) recorded during the same experiments as the 147 amu curves presented in Fig. 1. As shown previously [20], the desorption peaks above 55 K are also present in reference mixtures of HMDSO and CH_4 but their relative intensity as compared to the 55 K peak is higher than in HMDSO after electron exposure (Fig. 3). This suggests that the 55 K peak is due to CH_4 near the film surface while the higher temperature signals stem from CH_4 trapped within the HMDSO film and released upon thermally induced reorganisation of the film. The TDS curves presented in Fig. 2 show the energy dependence of CH_4 production. While a small signal near 160 K at all E_0 stems from HMDSO, signals due to CH_4 are observed after electron exposure at and above 11 eV. They become more pronounced as E_0 increases.

The results of Figs. 1 and 2 show that the reaction rate for decay of HMDSO and formation of CH_4 becomes noticeable between E_0 = 9 and 11 eV. The ionisation energy of gaseous HMDSO has been reported as 9.6 eV [21]. The threshold for the observed reactions thus corresponds roughly to the ionisation threshold. The observation that the decay of HMDSO is negligible below this threshold is in agreement with the results of Section 3.1 which show that formation of negative ions from gaseous HMDSO is not an efficient process in the energy range investigated here. In consequence, a resonant enhancement of HMDSO reactivity can also not be deduced from the condensed phase experiments.

3.3. Quantification of CH_4 formation in condensed HMDSO

In a previous work, the cross-section for degradation of HMDSO in molecular films exposed to electrons at 15 eV was estimated as 6×10^{-16} cm^2 for the degradation of the high-temperature peak and of 1.5×10^{-16} cm^2 for the low-temperature peak [16]. In order

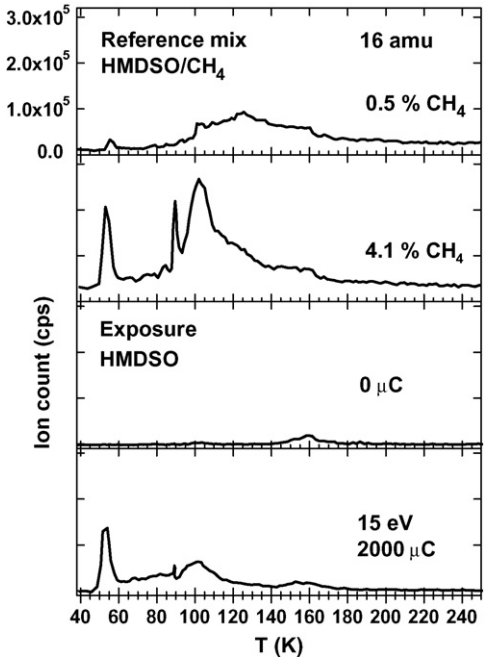

Fig. 3. Thermal desorption spectra recorded at 16 amu (CH_4^+) for non-exposed multilayer films of HDMSO/CH_4 reference mixtures deposited at 35 K from an amount of vapour corresponding to a pressure drop of 4.0 mTorr in the inlet system (top) and thermal desorption spectra before and after electron exposure of 2000 μC at 15 eV of HMDSO films prepared from the same amount of vapour.

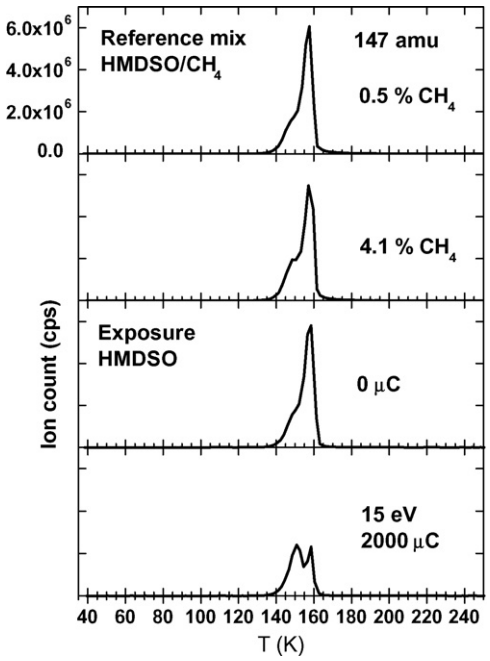

Fig. 4. Thermal desorption spectra recorded at 147 amu ($[HMDSO–CH_3]^+$, the dominant fragment mass of HMDSO) for non-exposed multilayer films of HDMSO/CH_4 reference mixtures deposited at 35 K (top) and thermal desorption spectra before and after electron exposure of 2000 μC at 15 eV of pure HMDSO films. The data stem from the same experiment as shown in Fig. 3.

to obtain more insight into the mechanism of this reaction, it is important to quantify the amount of the products as well.

Following the procedure described in detail previously [22], the amount of produced CH_4 is quantified at E_0 = 15 eV by comparing the integrated intensity of the desorption signal for CH_4 in the 16 amu TDS curve acquired after electron exposure to the integrated intensity of the same signal in reference mixtures of CH_4 and HMDSO containing specific amounts of CH_4. Fig. 4 demonstrates that this approach is justified because the absolute intensities in the exposure experiment (0 μC) and the TDS experiment with the reference mixtures (here: 0.5% and 4.1% CH_4) are approximately comparable as obvious from the very similar intensities of the HMDSO desorption signals in the 147 amu curves. As desorption of CH_4 proceeds over a wide temperature range (Fig. 3), the 16 amu (CH_4) desorption signal is integrated over the full temperature range in order to obtain a quantitative measure of the amount of CH_4 in the film.

The evolution of the integrated TDS intensities as measured at 16 amu, i.e., of CH_4, in the exposure experiment is compared to the values obtained from the reference mixtures in Fig. 5. As expected, the integrated intensity of the reference mixtures shows an approximately linear increase with percentage of CH_4 within the film. Comparing the intensities obtained after exposure with the linear fit to the reference data, we deduce that the amount of CH_4 produced in HMDSO under electron exposure reaches only about 2% at 2000 μC. At the same time, about half of the HMDSO has disappeared as obvious from Fig. 4. This finding is discussed in Section 3.5 in relation to a possible reaction mechanism.

3.4. Formation of other products in condensed HMDSO under electron exposure at 15 eV

As the amount of produced CH_4 (Fig. 2) and the loss of HMDSO (Fig. 1) are strongest at E_0 = 15 eV, attempts to identify other products were restricted to this energy. Different masses were monitored, including, besides 147 and 16 amu characteristic of HMDSO and CH_4, 73 amu (characteristic of various organosilicon compounds), 30 amu (ethane, C_2H_6), as well as some other mass peaks expected for larger saturated hydrocarbons. In addition to CH_4, more products resulting from electron exposure at 15 eV were observed in the 30, 147, and 73 amu curves (Fig. 6). Other investigated masses did not provide further information. Compared to the data shown in Figs. 3–5, the experiments of Fig. 6 were performed at somewhat smaller film thickness. Nonetheless, the intensity of the desorption signals of the products was closely comparable between the two sets of experiments. This most probably reflects the limited penetration depth of electrons within the films. We therefore use the data shown in Fig. 6, in the following, to obtain a crude estimate of the amount of the products other than CH_4.

Fig. 6(a) shows that, besides CH_4, C_2H_6 is formed, as again identified by its desorption temperature (75–80 K [17]). Note that the signal between 140 and 165 K in the 30 amu curve stems from HMDSO. While comprehensive measurements of reference mixtures were not performed for C_2H_6, an estimate of its quantity can still be obtained using cross-sections for dissociative electron impact ionisation at 70 eV producing CH_3^+ from CH_4 (0.38×10^{-16} cm^2) and from C_2H_6 (0.5×10^{-17} cm^2) [9] and the relative intensities of CH_3^+ and $C_2H_6^+$ in mass spectrum of C_2H_6 and of CH_3^+ and CH_4^+ in the spectrum of CH_4 obtained with electron impact ionisation at the same electron energy [21]. From this we estimate that the 16 amu signal from CH_4 should be about 1.5 times more intense than the 30 amu signal from C_2H_6. By comparing the intensities of the desorption peaks in the 16 and 30 amu TDS curves after an exposure of 2000 μC (Figs. 3 and 6a) we deduce that at least 20–30 times more CH_4 is produced than C_2H_6.

Mass 73 amu is also a strong signal of HMDSO, thus the shape of the strong desorption signal between 140 and 165 K also follows that of the 147 amu curve over the same temperature range (Fig. 6b and c). An additional weak peak at 128 K is observed for the non-exposed sample. As this signal does not occur in the 147 amu curve, it cannot be due to HMDSO but probably relates to an unidentified minor impurity. New signals in the 73 amu curve observed after an exposure of 2000 μC are located at 115 and 205 K. The desorption signal at 115 K is clearly assigned to tetramethylsilane (TMS) based on a comparison with the desorption temperature of TMS in a mixed HMDSO/TMS film (Fig. 7). Using this reference mixture of HMDSO containing 3.9% TMS, the amount of TMS present after an electron exposure of 2000 μC can be estimated. The 73 amu TDS curve of the

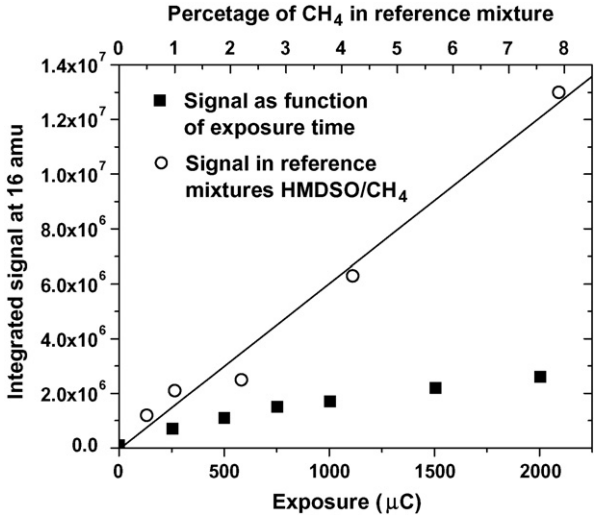

Fig. 5. Plot of the integrated desorption signal for 100 data points (roughly 40–210 K) recorded at 16 amu as function of electron exposure at 15 eV and plot of the same integrated intensity for reference mixtures as function of CH_4 content. The data stem from the same experiment as shown in Figs. 3 and 4.

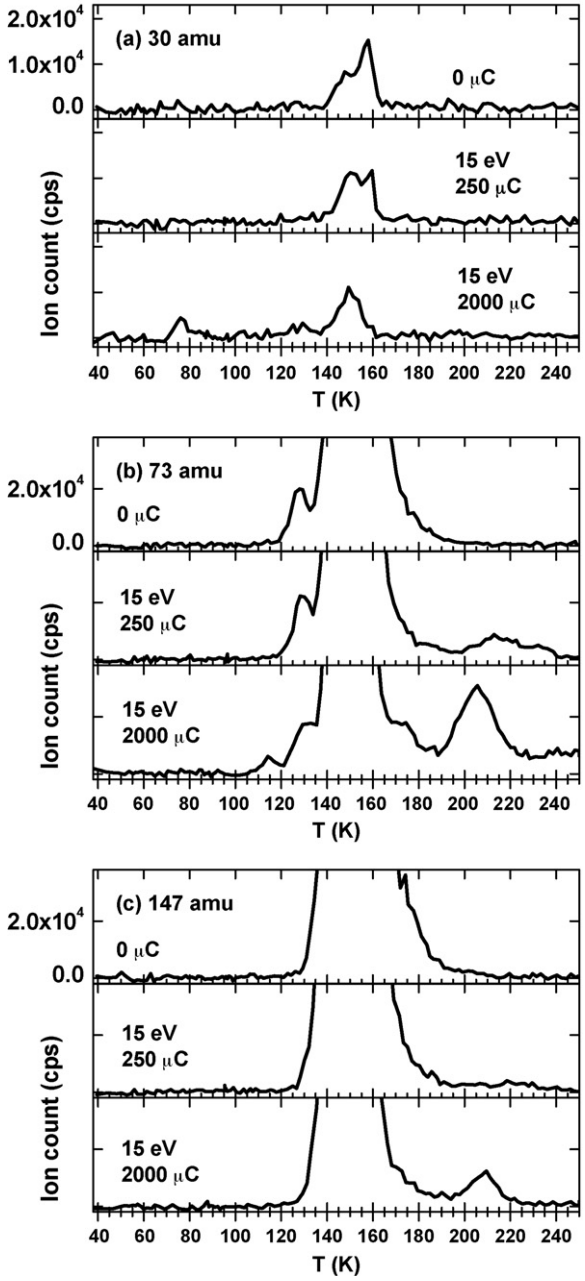

Fig. 6. Thermal desorption spectra recorded at (a) 30 amu ($C_2H_6^+$ or SiH_2^+), (b) 73 amu ($Si(CH_3)_3^+$), and (c) 147 amu ($[HMDSO–CH_3]^+$) for a non-exposed multilayer film of HMDSO deposited at 35 K from an amount of vapour corresponding to a pressure drop of 3.0 mTorr in the inlet system and films prepared in the same way after different electron exposures at E_0 = 15 eV.

reference mixture shows an intensity ratio of 10:100 between the desorption peaks at 115 K (TMS) and 158 K (HMDSO). This ratio is roughly consistent with the fact that the gas-phase cross-sections for dissociative ionisation of TMS yielding $[TMS–CH_3]^+$ (73 amu) and of HMDSO yielding $[HMDSO–CH_3]^+$ (147 amu) are very similar [12,23] and the 73 amu signal has about 43% of the intensity of the 147 amu signal for HMDSO in the present experiments. After an exposure of 2000 μC onto an initially pure HMDSO film the intensity ratio between the peaks at 115 and 158 K is 0.5:100. Taking furthermore into account that the HMDSO signal has decreased to approximately 54% of its value prior to exposure, the TMS signal corresponds to roughly 0.1% TMS relative to the original amount of HMDSO. Similar to the case of CH_4 where desorption occurs over a wide temperature range, TMS may be trapped in the HMDSO film and be released upon desorption of HMDSO. If this contribution was significant, the intensity ratio of the desorption peaks between 140 and 160 K in the TDS curves for 147 and 73 amu would be different before and after electron exposure. In fact, this value changes from 0.43 for pure HMDSO to 0.46 after an exposure of 2000 μC. Following the same arguments as for the 115 K desorption signal we deduce that a maximum amount of 5% TMS as compared to the original amount of HMDSO may desorb together with the remaining HMDSO.

As discussed in detail previously [20], the desorption temperature of a product which desorbs at higher temperature than the majority component of the molecular film (here: HMDSO) is more difficult to predict from reference experiments. In a film of HMDSO only a few monolayers thick and containing up to a few percent of a larger siloxane, the coverage of the larger siloxane after desorption of HMDSO varies in the submonolayer to monolayer regime and the desorption temperature thus shifts with the percentage of the larger siloxane. If, after electron exposure, further products with still higher desorption temperature (i.e., longer oligomers) are present, they may form a matrix from which the investigated product may again desorb at a constant temperature. Therefore, the assignment of the desorption signal occurring at 205 K after 2000 μC in the 73 amu TDS curve is not as straightforward as for TMS. The signal is located at somewhat higher desorption temperature after 250 μC (215 K) as characteristic for a small quantity. On the other hand, evidence for the presence of other products is also found in the 147 amu TDS curve (Fig. 6). After an exposure of 2000 μC, a new desorption signal appears at 210 K and thus at a slightly higher temperature than in the 73 amu curve. This suggests that at least a second product with similar size is formed. Furthermore, a previous study has shown that some material remains on the substrate after a TDS run with maximum temperature of 270 K [16]. This material certainly influences the exact desorption temperature of the lower mass products.

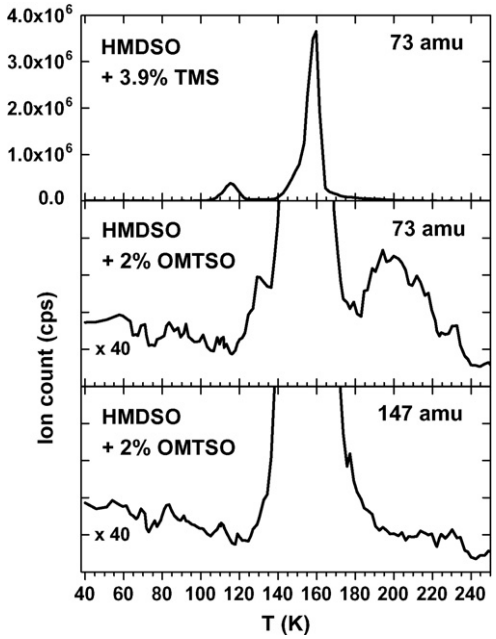

Fig. 7. Thermal desorption spectra recorded at 73 amu ($Si(CH_3)_3^+$) for a non-exposed HMDSO film mixed with 3.9% TMS and recorded at 73 amu and 147 amu ($[HMDSO–CH_3]^+$) and for a non-exposed film of HMDSO mixed with 2% OMTSO. Both films were deposited at 35 K from an amount of vapour corresponding to a pressure drop of 4.0 mTorr in the inlet system.

As 73 amu is a characteristic signal of siloxanes and the desorption temperature is higher than that of HMDSO, we suggest that a larger siloxane is formed. For comparison, reference mixtures of HMDSO and octamethyltrisiloxane (OMTSO) were investigated. Fig. 7 shows a representative result for HMDSO containing 2% OMTSO. As the molecular mass of octamethyltrisiloxane (OMTSO) exceeds the mass range of the presently used QMS we rely on the 73 amu fragment for its identification. Contrary to literature mass spectra also obtained with electron impact ionisation at 70 eV but in accord with data for larger siloxanes from the same source [21], a 147 amu signal is not observed for OMTSO in the present measurements. The desorption rate of OMTSO for the mixed film reaches its maximum at a temperature of 200 K. This is slightly lower than for the product formed in HMDSO. Additional experiments revealed that the desorption temperature of pure OMTSO films shifts strongly with coverage from 220 K at submonolayer to 175 K for the multilayer. Based on the rather similar desorption temperature we suggest tentatively that a siloxane product containing three silicon atoms is formed. More comprehensive reference experiments are nonetheless required to obtain an unequivocal assignment. Consequently, an estimate of the quantity of this product is not undertaken here.

3.5. Implications for reaction mechanisms

The results clearly show that HMDSO films are efficiently modified by exposure to electrons at $E_0 = 15$ eV. After an exposure of 2000 μC, about 50% of the initial amount of HMDSO has disappeared, a so far unquantified amount of larger siloxanes as well as 2% CH_4 and up to 5% TMS are formed besides small quantities (<0.1%) of C_2H_6. This section reviews possible mechanisms for these reactions and discusses their suitability to rationalize the detected amounts of the products.

3.5.1. Initiating reaction (Scheme 1)

Electron interaction with HMDSO initiates further reactions by producing reactive fragments. The gas-phase results provide evidence concerning the most likely dissociation channel. Previous studies on electron-induced reactions of gaseous HMDSO [12,19,24] and on the composition of HMDSO plasmas [6] have shown that electron impact ionisation at low electron energies predominantly leads to the formation of a pentamethyldisiloxane (PMDSO) cation and a CH_3 radical (Scheme 1). The gas-phase cross-section of 4.0×10^{-16} cm^2 at $E_0 = 15$ eV [12] shows that this is an efficient process. The present gas-phase results, in addition, show that electron interaction with HMDSO at E_0 up to 15 eV does not produce measurable amounts of negative ions other than perhaps H^- which was not accessible with the presently used apparatus. Also, measurements on electron-stimulated desorption (ESD) of negative ions from condensed HMDSO have not been reported so far. Evidence for DEA as well as for DD within this energy range is thus missing. We therefore assume that the reaction shown in Scheme 1 is the dominant initial reaction step in condensed HMDSO under exposure to low-energy electrons. Both the PMDSO cation and the CH_3 radical may undergo subsequent reactions with adjacent HMDSO molecules as summarized in Schemes 2 and 3.

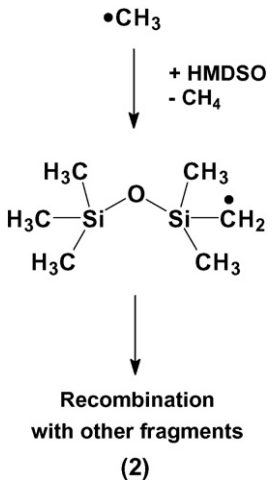

Scheme 2.

3.5.2. Radical reactions (Scheme 2)

A previous study on electron-induced reactions in condensed acetonitrile (CD_3CN) has shown that CD_3 radicals produced under electron exposure abstract D atoms from adjacent molecules to form CD_4 [17]. In fact, CD_3H was not produced which clearly demonstrated that formation of methane is not due to recombination of the radical with residual gas in the vacuum chamber. The same can thus be safely assumed for the present experiments on HMDSO. Formation of CH_4 must therefore result from the reaction shown in Scheme 2. Recombination of the resulting [HMDSO–H] radicals with other fragments, including possibly cationic species neutralized by thermalized electrons within the film, is one possible pathway leading to larger siloxanes.

It must be noted that attempts to find evidence for the formation of a $–CH_2–$ bridge by means of reflection absorption infrared spectroscopy (RAIRS) were not successful. This group should exhibit a characteristic band near 1360 cm^{-1} which has been observed in plasma polymerisation of HMDSO [8]. On the other hand, it is relatively weak and consequently difficult to identify with certainty if the mixture contains only small amounts of this product as suggested by the detected quantity of CH_4.

CD_3 radicals in acetonitrile films were also observed to efficiently recombine producing C_2D_6 [17]. Acetonitrile was found to decay with similar efficiency as HMDSO but CD_4 and C_2D_6 were produced in comparable quantities. This results from a comparison of the relevant desorption peak intensities and by use of the same arguments as described in Section 3.3. The very low yield of

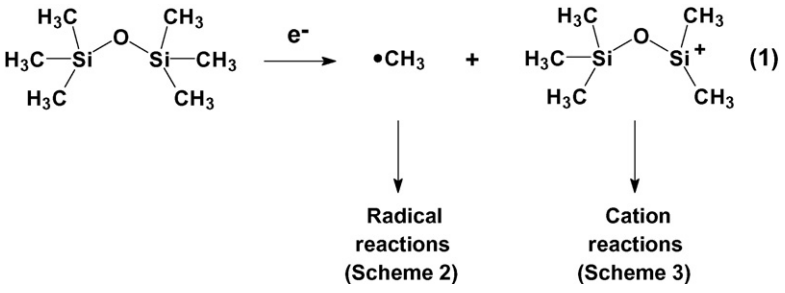

Scheme 1.

C_2H_6 observed in condensed HMDSO thus points towards a relatively low mobility of CH_3 radicals in the HMDSO films in accord with the observed trapping of CH_4 (Section 3.2). The bulky HMDSO molecules thus appear to prevent CH_3 radicals from approaching each other. This also suggests that recombination reactions most probably occur locally, i.e., between adjacent molecules with suitable orientation, or just before desorption, i.e., when a sufficient mobility is reached.

3.5.3. *Cation reactions (Scheme 3)*

If the reactions shown in Schemes 1 and 2 were the dominant reactions, two HMDSO molecules would decay per CH_4 formed. This ratio is by an order of magnitude different from the one deduced from the present experiments. Reactions initiated by the PMDSO cation may, on the other hand, remove more HMDSO. In fact, gas-phase studies of ion-molecule reactions have revealed that PMDSO cations can react with HMDSO to form an intermediate with trivalent and positively charged oxygen as shown in Scheme 3 [12]. It was also shown that this intermediate could release TMS to yield a longer linear siloxane cation. In the condensed phase this sequence may, in principle, be repeated as elementary steps of a cationic polymerisation reaction (Route 3a). On the other hand, if this were the dominant reaction in the present experiments, each HMDSO consumed via the chain growth reaction of route (3a) would yield one TMS. In fact, a maximum amount of one TMS is observed per ten molecules of HMDSO that decay. Including the initiating reaction (1), assuming that it is generally followed by consumption of another HMDSO via reaction (2) and that polymerisation stops after the steps shown in Scheme 3, one TMS would be formed per three instead of ten decomposed molecules of HMDSO. This suggests that other reaction sequences consuming HMDSO must exist. In the context of HMDSO plasma polymerisation, it was suggested that the intermediate $Si_4O_2(CH_3)_{11}^+$ may also decay by expulsion of a $Si(CH_3)_3^+$ to yield OMTSO [25]. This reaction which is reminiscent of Lewis acid catalysed equilibration of siloxanes [26] provides an alternative pathway to decay of HMDSO (Route 3b). With respect to the gas-phase where it was shown that $Si(CH_3)_3^+$ reacts with HMDSO to form again a PMDSO cation and TMS [12], this cation may be trapped and stabilized in the condensed phase by forming an adduct with HMDSO. Still, this reaction is not a satisfactory explanation for decay of HMDSO without or with little production of TMS and CH_4 because it does not start a chain reaction. The reaction cannot proceed because the intermediate can only decay either back to HMDSO and $Si(CH_3)_3^+$ or to a PMDSO cation and TMS, with the PMDSO cation starting the reaction sequence of Scheme 3 again. On the whole, again, decay of HMDSO would either not be extensive or lead to production of important amounts of TMS in conflict with the present findings. Finally, the gas-phase cross-sections for dissociative ionisation leading to abstraction of CH_3 radicals are very similar for HMDSO and TMS [12,23]. TMS can thus be fragmented with similar efficiency as HMDSO. Still, even if TMS itself is consumed by electron-driven processes implying at the same time that the reactions leading to its formation (Scheme 3) take place at low temperature, the resulting fragments would again contribute to the reactions already included in Schemes 2 and 3 and leading to production of more TMS.

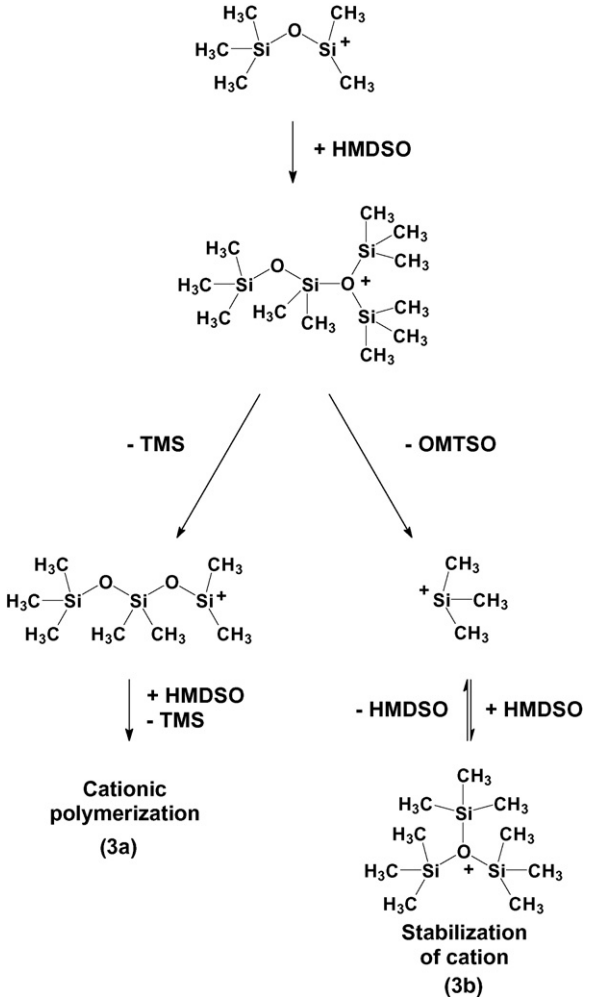

Scheme 3.

As the survey of reaction mechanisms suggested in literature fails to explain the relative extent of HMDSO decomposition and CH_4 and TMS production, alternative reaction pathways need to be identified. So far, it has not been investigated if HMDSO may be removed from the surface via ESD. On the other hand, a previous study on electron-induced reactions in acetaldehyde molecular films [22] has shown that important amounts of CO produced under irradiation at E_0 = 15 eV are retained within the molecular film at the temperature of the present exposure experiments. The amount of CO that is detected by TDS reflects about half of the decomposed acetaldehyde even if its desorption temperature is only slightly higher than the temperature at which exposure was performed. In the light of these results it appears unlikely that an important fraction of HMDSO, which has a much higher desorption temperature, can in fact be removed by electron-induced desorption. Nonetheless, this possibility will be investigated in a forthcoming study.

Finally, the possibility that DEA producing H^- may occur within the molecular film cannot be fully excluded so far due to a lack of measurements on ESD of negative ions. Such a reaction would yield a [HMDSO–H] radical that could form larger siloxanes by recombination with other radicals without necessarily producing CH_4 or TMS. DEA producing H^- is an efficient process at E_0 near 10 eV in saturated hydrocarbons [27,28]. Therefore, it is possible that the methyl periphery of HMDSO may also undergo such a reaction under exposure if electrons are slowed down somewhat inside the film. ESD measurements on HMDSO condensed films are needed to solve this question.

4. Conclusions

Electron-induced reactions in films of HMDSO deposited on a Au substrate at a temperature of 35 K have been monitored by thermal desorption spectrometry for electron energies ranging from 5 to 15 eV and the products were investigated at 15 eV. HMDSO is efficiently consumed but surprisingly small amounts of low-mass products (CH_4, C_2H_6, and TMS) have been detected. The

electron-induced dissociative ionisation of HMDSO leading to a pentamethyldisiloxane cation and a CH_3 radical very likely initiates further reaction steps that can lead to formation of longer siloxanes with a cationic polymerisation mechanism or reactions reminiscent of the Lewis acid catalysed equilibration of siloxanes. The low yield of C_2H_6 as compared to other previously studied systems points towards a hindered mobility of fragments within the HMDSO film so that formation of CH_4 by abstraction of an H atom from an adjacent HMDSO is the more important reaction channel for CH_3 radicals. The observation that the yield of TMS is low compared to that expected for the anticipated cationic polymerisation hints towards the existence of other decay channels for HMDSO. Upcoming investigations therefore will aim at measurements of electron-induced desorption as well as more extensive reference experiments to arrive at a more precise identification of the larger siloxane products observed in the present study.

Acknowledgements

Support provided by the Volkswagen Foundation under grant "Plasma hybrid coatings: functional surfaces by plasma supported nanotechnology" and by COST Action CM0601 "Electron Controlled Chemical Lithography" (ECCL) is gratefully acknowledged.

References

[1] W. Geyer, V. Stadler, W. Eck, M. Zharnikov, A. Gölzhäuser, W. Grunze, Appl. Phys. Lett. 75 (1999) 2401.
[2] W. Eck, V. Stadler, W. Geyer, M. Zharnikov, A. Gölzhäuser, M. Grunze, Adv. Mater. 12 (2000) 805.
[3] W. Di, P. Rowntree, L. Sanche, Phys. Rev. B 52 (1995) 16618.
[4] A. Lafosse, M. Bertin, D. Caceres, C. Jäggle, P. Swiderek, D. Pliszka, R. Azria, Eur. Phys. J. D 35 (2005) 363.
[5] H. Abdoul-Carime, S. Gohlke, E. Illenberger, Phys. Rev. Lett. 92 (2004) 168103; S. Ptasińska, S. Denifl, V. Grill, T.D. Märk, P. Scheier, S. Gohlke, M.A. Huels, E. Illenberger, Angew. Chem. Int. Ed. 44 (2005) 1647; S. Ptasińska, S. Denifl, V. Grill, T.D. Märk, E. Illenberger, P. Scheier, Phys. Rev. Lett. 95 (2005) 093201; S. Ptasińska, S. Denifl, P. Scheier, E. Illenberger, T.D. Märk, Angew. Chem. Int. Ed. 44 (2005) 6941.
[6] D. Magni, C. Deschenaux, C. Hollenstein, A. Creatore, P. Fayet, J. Phys. D 34 (2001) 87.
[7] P. Raynaud, B. Despax, Y. Segui, H. Caquineau, Plasma Process. Polym. 2 (2005) 45.
[8] C. Rau, W. Kulisch, Thin Solid Films 249 (1994) 28.
[9] K. Li, O. Gabriel, J. Meichsner, J. Phys. D 37 (2004) 588.
[10] F. Benítez, E. Martínez, J. Esteve, Thin Solid Films 377–378 (2000) 109.
[11] M.R. Alexander, F.R. Jones, R.D. Short, Plasma Polym. 2 (1997) 277.
[12] C.Q. Jiao, C.A. De Joseph, A. Garscadden, J. Vac. Sci. Technol. A 23 (2005) 1295.
[13] P. Kurunczi, A. Koharian, K. Becker, K. Martus, Contr. Plasma Phys. 36 (1996) 723.
[14] P. Kurunczi, K. Becker, K. Martus, Can. J. Phys. 76 (1998) 153.
[15] C. Danelon, C. Santschi, J. Brugger, H. Vogel, Langmuir 22 (2006) 10711.
[16] I. Ipolyi, P. Swiderek, Surf. Sci. 602 (2008) 3199.
[17] I. Ipolyi, W. Michaelis, P. Swiderek, Phys. Chem. Chem. Phys. 8 (2007) 182.
[18] S. Matejcik, I. Ipolyi, E. Illenberger, Chem. Phys. Lett. 375 (2003) 660.
[19] S. Carles, J.L. Le Garrec, J.B.A. Mitchell, J. Chem. Phys. 127 (2007) 144308.
[20] E. Burean, I. Ipolyi, T. Hamann, P. Swiderek, Int. J. Mass Spectrom. 277 (2008) 215.
[21] NIST Chemistry Web Book, NIST Standard Reference Database Number 69, Eds. P.J. Linstrom and W.G. Mallard, June 2005, National Institute of Standards and Technology, Gaithersburg, MD, 20899 (http://webbook.nist.gov).
[22] E. Burean, P. Swiderek, Surf. Sci. 602 (2008) 3194.
[23] R. Basner, R. Foest, M. Schmidt, F. Sigeneger, P. Kurunczi, K. Becker, H. Deutsch, Int. J. Mass Spectrom. Ion Proc. 153 (1996) 65.
[24] R. Basner, R. Foest, M. Schmidt, K. Becker, H. Deutsch, Int. J. Mass Spectrom. 176 (1998) 245.
[25] A.M. Wrobel, M. Kryszewski, M. Gazicki, J. Macromol. Sci. A 20 (1983) 583.
[26] C.J. Embery, J.G. Matisons, S.R. Clarke, Synthesis and properties of silicones and silicone-modified materials, in: S.J. Clarson, J.J. Fitzgerald, M.J. Owen, S.D. Smith, M.E. van Dyke (Eds.), ACS Symposium Series, 2003, p. 26.
[27] P. Rowntree, L. Parenteau, L. Sanche, J. Phys. Chem. 95 (1991) 4902.
[28] C. Olsen, P. Rowntree, J. Chem. Phys. 108 (1998) 3750.